Dynamic characteristics of resonant gyroscopes study based on the Mathieu equation approximate solution*

Fan Shang-Chun(樊尚春), Li Yan(李 艳)†, Guo Zhan-She(郭占社), Li Jing(李 晶), and Zhuang Hai-Han(庄海涵)

School of Instrument Science & Opto-electronics Engineering, Beihang University, Beijing 100191, *China*
Key Laboratory of Precision Opto-mechatronics Techonology of Ministry of Education, Beijing 100191, *China*
Key Laboratory of Inertial Science and Technology for National Defence, Beijing 100191, *China*

(Received 10 June 2011; revised manuscript received 15 November 2011)

Dynamic characteristics of the resonant gyroscope are studied based on the Mathieu equation approximate solution in this paper. The Mathieu equation is used to analyze the parametric resonant characteristics and the approximate output of the resonant gyroscope. The method of small parameter perturbation is used to analyze the approximate solution of the Mathieu equation. The theoretical analysis and the numerical simulations show that the approximate solution of the Mathieu equation is close to the dynamic output characteristics of the resonant gyroscope. The experimental analysis shows that the theoretical curve and the experimental data processing results coincide perfectly, which means that the approximate solution of the Mathieu equation can present the dynamic output characteristic of the resonant gyroscope. The theoretical approach and the experimental results of the Mathieu equation approximate solution are obtained, which provides a reference for the robust design of the resonant gyroscope.

Keywords: resonant gyroscopes, dynamic characteristics, Mathieu equation, approximate solution

PACS: 04.40.Dg, 02.30.Hq, 05.10.–a **DOI:** 10.1088/1674-1056/21/5/050401

1. Introduction

Resonance is a property of a system, which describes an enhanced response at a certain characteristic frequency that is wholly determined by parameters of the system.[1] The specific frequency is the one at which the system retains the input energy with minimum loss. At the microscopic scale, the resonance enhances the effect of small force and the device signal-to-noise ratio. Operation at resonance is advantageous not only for micromechanical actuators but also for sensing. The resonant sensing often involves the detection of input by means of resonant frequency shift of the sensing device. In applications such as the gyroscope that require large amplitude motions, operation at resonance is highly desirable.

A resonant gyroscope operates based on the principle of detecting an induced Coriolis acceleration on a vibrating proof mass in the presence of an applied rotation rate, as its name implies. In the resonant gyroscope, the resonant sensing serves as the basis for the Coriolis force detection. The detection of frequency shift is more advantageous than that of change in amplitude, as it is less sensitive to effects such as feedthrough couplings from undesired sources and parasitic passive elements. The resonant gyroscope technique also benefits from being highly sensitive, low noise, and potentially low power and having large dynamic range and good linearity.

Although the gyroscopes have been the subject of intensive research in the past few years,[2–5] and the resonant gyroscope possesses the above advantages, there is not much research on it and its dynamic characteristics. Seshia *et al.*[6] reported an integrated microelectromechanical resonant gyroscope, but they did not give the dynamic characteristics of the resonant gyroscope in detail. Hassan and Roger[7] reported the theory of direct frequency output vibratory gyroscope, but they were concerned with the gyroscope whose vibratory mode was out of plane, and the detection principle was not resonant sensing that measured the Coriolis force directly. There are some other investigations about the resonant gyroscope, but they all focus on the driving control or the fabrication process.[8–10] The gyroscope with resonant output has not been fab-

*Project supported by the National Natural Science Foundation of China (Grant No. 60927005), the Innovation Foundation of BUAA for Ph. D. Graduates, China, and the Fundamental Research Funds for the Central Universities, China (Grant No. YWF-10-01-A17).

†Corresponding author. E-mail: yanli.83@163.com

© 2012 Chinese Physical Society and IOP Publishing Ltd

ricated commercially. The main reason is that the resonant gyroscope develops slowly due to the fact that the Mathieu equation has not been solved completely. The Mathieu equation is a differential equation, which can be used to describe the dynamic characteristics of the resonant gyroscope.

The Mathieu equation is an excellent paradigm for studying the parametric resonance (PR), which is a subharmonic resonance that exemplifies the response of a system to a kind of periodic force. In fluid dynamics, many examples of waves may be excited by the PR. Other examples can be found in acoustic instabilities of flames[11] and the Rayleigh–Benard convection.[12] In geophysical fluid dynamics, Poulin *et al.*[13] and Pedlosky and Thomson[14] derived ordinary differential equations of the Hill type to describe the stabilities of barotropic and baroclinic shear flows, respectively. The Mathieu equation is also important for describing travelling waves in a spatially uniform medium. However, there have not been any reports about parametric resonant dynamic characteristics in resonant gyroscopes.

Finding the space of parameters is very important for finding a stable approximate solution of the Mathieu equation. Hence, it is of interest to characterize the dynamic characteristics by a stable approximate solution of the Mathieu equation. Recently, several authors have studied stable approximate solutions for the Mathieu equation,[15−18] but the approximate solutions they obtained are very complicated and just reflect the parameter resonant excitement stability under some conditions; several other authors have studied the stability of the Mathieu equation approximate solution[19−21] to find out the stable state in the parametric periodic excitement, but they did not give any clear approximate solution. All the studies mentioned above only concern with the mathematical analysis, the results have no practical values and may not be used directly to analyse the dynamic characteristics of resonant gyroscopes.

In this paper, we solve the problems mentioned above for resonant gyroscopes. We use an approximate solution to study the dynamic characteristics of resonant gyroscopes. First of all, we introduce the parametric resonant characteristics based on the resonant gyroscope working principle, and study the relations between the Mathieu equation and the parametrical resonant characteristics of the resonant gyroscope. Then we use the method of small parameter perturbation, simulate and discuss the approximate solution of the Mathieu equation with the fluctuation of parameters for the resonant gyroscope. Finally, in order to verify the validity of the approximate solution for the Mathieu equation, simulations and experiments are performed.

2. Mathematical modeling

2.1. Working principle of resonant gyroscope

A schematic diagram of the z-axis resonant gyroscope is shown in Fig. 1. The proposed gyroscope dynamical system consists of a sense-mode oscillator and a drive-mode oscillator. The proof mass is free to oscillate in the sense direction, and is excited in the drive direction. In the drive direction, the proof mass oscillates and behaves as a resonant oscillator. For a given z-axis Ω, the Coriolis force acts on the proof mass, then the sense-mode system transmits this force into two double ended tuning fork (DETF) resonators placed on each side to provide a differential output. The two tines of the tuning forks vibrate in anti-phase to each other. The periodic compression and tension of the tuning fork tines, which are induced by the action of the Coriolis force on the proof mass, modulate the resonant frequency of the DETF. Each force sensor is comprised of the mechanical structure of tuning fork embedded in the feedback loop of an oscillator circuit.

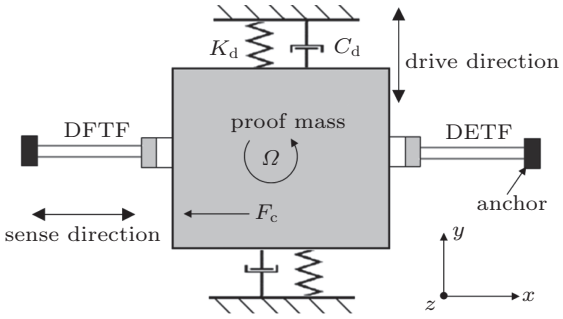


Fig. 1. Simplified model of the resonant gyroscope.

2.2. Modeling

As mentioned above, the drive mode of the resonant gyroscope is a one-dimensional dynamic system, the operational frequency can be achieved by adjusting the drive mode stiffness or the decoupling frame mass, and the drive mode is independent of the sense mode. Therefore, the focus of the resonant gyroscope is on the DETF sense mode, specifically on demodulating the oscillator output frequency.

The resonant gyroscope has two sets of DETF resonators serving as the angular velocity sensors, the push and the pull resonators. Each resonator is formed with two beams. The two DETF resonators are excited simultaneously by two oscillators and vibrate at their resonant frequency. For each mode of vibration, the input of the drive oscillator is connected to the detection devices, and the output to the driving devices. When the resonant gyroscope has an angular velocity, the resonant frequencies of the two DETF resonators vary with the angular velocity due to the Coriolis effect. The Coriolis force will cause axial push and pull loadings on the DETF resonators to shift their resonant frequency. One DETF resonator is subjected to a tension due to the pull axial loading, thus the resonant frequency will increase. The other DETF will be under compression, and the frequency will decrease. As a result, the difference in the resonance frequency between the two modes is a function of the applied angular velocity, and the frequency shifts of the two resonators are proportional to the applied angular velocity input. Figure 2 shows the operating principle of the DETF.

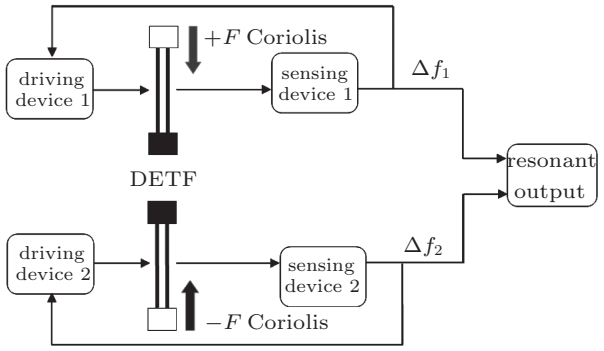


Fig. 2. Schematic diagram of the operating principle of DETF.

The dynamics of the device can be described by a series of coupled differential equations. The proof mass dynamics can be described by classical spring–mass–damper equations. The dynamics of the DETF subjected to an axial time-varying Coriolis force is given by the parametric excitement equation.

The free DETF dynamic equation can be expressed as

$$EI\frac{\partial^4 w}{\partial x^4}+\xi\frac{\partial w}{\partial t}+F\frac{\partial^2 w}{\partial x^2}+\rho A\frac{\partial^2 w}{\partial t^2}=0, \tag{1}$$

where E is the Young's modulus of elasticity, I is the moment of inertia, $F(t)$ is the total instantaneous axial load expressed as

$$F(t)=F_0\cos(\omega_{\rm d}t), \tag{2}$$

with $\omega_{\rm d}$ being the resonant frequency of the proof mass. The boundary conditions are $w=0$, $\frac{\partial w}{\partial x}=0$ at $x=0,L$. The equation of motion governing the transverse vibration ($w(x,t)=\phi(x)q(t)$) as a function of position x along the length of the beam at time t is given by Eq. (1), where $\phi(x)$ is the mode-shape function, $q(t)$ is the response of the vibratory track with time. Substituting the above function into Eq. (1) leads to the following equation:

$$\int_0^L \rho A\phi^2\,{\rm d}x\ddot{q}+\int_0^L \xi\phi^2\,{\rm d}x\dot{q} +\left(\int_0^L EI\left(\frac{\partial^2\phi}{\partial x^2}\right)^2{\rm d}x+\int_0^L F\left(\frac{\partial\phi}{\partial x}\right)^2{\rm d}x\right)q=0. \tag{3}$$

Because the DETF working under 1 mode ($i=1$) satisfies these conditions, the no-load resonant angular frequency ω_0 and the instantaneous frequency ω_n of the DETF can be obtained as

$$\omega_0=\sqrt{\int_0^1\frac{EI}{L^3}\left(\frac{\partial^2\phi}{\partial\tau^2}\right)^2{\rm d}\tau\Big/\int_0^1\rho AL\phi^2\,{\rm d}\tau}=\left(\frac{4.730}{L}\right)^2\sqrt{\frac{EI}{\rho A}}, \tag{4}$$

$$\omega_n=\sqrt{\left[\int_0^1\frac{EI}{L^3}\left(\frac{\partial^2\phi}{\partial\tau^2}\right)^2{\rm d}\tau+\int_0^1\frac{F}{L}\left(\frac{\partial\phi}{\partial\tau}\right)^2{\rm d}\tau\right]\Big/\int_0^1\rho AL\phi^2\,{\rm d}\tau}=\omega_0\sqrt{1+\frac{0.293FL^2}{12EI}}. \tag{5}$$

Under driving force $F_{\rm d}$, the DETF works at its resonant frequency, and the dynamic equation can be expressed as

$$\int_0^L \rho A\phi^2\,{\rm d}x\ddot{q}+\int_0^L \xi\phi^2\,{\rm d}x\dot{q}+\left[\int_0^L EI\left(\frac{\partial^2\phi}{\partial x^2}\right)^2{\rm d}x+\int_0^L F\left(\frac{\partial\phi}{\partial x}\right)^2{\rm d}x\right]q=F_{\rm d}. \tag{6}$$

The driving force $F_{\rm d}$ keeps the DETF working at the resonant frequency, so

$$\int_0^L \xi\phi^2 \,{\rm d}x\dot{q} = F_{\rm d}, \tag{7}$$

$$\ddot{q}(t) + \omega_0^2 \left(1 + \frac{0.293L^3F_0\cos\omega_{\rm d}t}{EI}\right) q(t) = 0. \tag{8}$$

If the transformations are chosen appropriately, equation (8) can be converted into a standard form. Let $\delta' = \omega_0^2$ and $\varepsilon' = \omega_0^2(0.293L^3F_0/2EI)$, equation (8) can be rewritten as

$$\ddot{q} + (\delta' + \varepsilon'\cos\omega_{\rm d}t)\, q = 0. \tag{9}$$

In order to use the method of small parameter perturbation, differential equation (9) is converted into a standard form for the parametric resonance. Let

$$\begin{cases} z = \dfrac{\omega_{\rm d}t}{2}, \\ q'' = \dfrac{{\rm d}^2q}{{\rm d}z^2}, \\ \delta = \delta'\left(\dfrac{2}{\omega_{\rm d}}\right)^2 = 4\left(\dfrac{\omega_0}{\omega_{\rm d}}\right)^2, \\ S = \dfrac{0.293L^3}{2EI}, \\ \varepsilon = 2\varepsilon'\left(\dfrac{2}{\omega_{\rm d}}\right)^2 = 4\left(\dfrac{\omega_0}{\omega_{\rm d}}\right)^2 \dfrac{0.293L^3F_0}{2EI}, \\ \quad = 4\left(\dfrac{\omega_0}{\omega_{\rm d}}\right)^2 SF_0, \\ F_0 = 2m\Omega\omega_{\rm d}A_{\rm m}, \end{cases} \tag{10}$$

where Ω is the input angular velocity, $A_{\rm m}$ is the maximum driving amplitude of the proof mass, and m is the mass of the proof mass, equation (9) becomes

$$q''(z) + (\delta + \varepsilon\cos 2z)\, q(z) = 0. \tag{11}$$

Equation (11) is known as the standard Mathieu equation. According to Eq. (11), the DETF vibration stiffness $k = \delta + \varepsilon\cos 2z$ changes with the Coriolis force exerted on the sensing mass of the resonant gyroscope. When the equivalent mass maintains the same, the DETF resonant frequencies will be changed accordingly. Here, parameter δ represents the DETF natural resonant frequency. The significant perturbation term $\varepsilon\cos 2z$, which represents the modulation of the spring constant of the resonant sensor at the proof mass driving frequency $\omega_{\rm d}$, is directly contributed by the Coriolis force exerted axially on the resonator tines.

Equation (11) exactly represents the parametric excitement dynamic characteristic of the resonant gyroscope. This equation has been widely studied in the context of parametric resonance, and the approximate solution of the Mathieu equation can be either bounded or unbounded, which is dependent on the parameters of the equation. This leads to the remarkable result that the approximate solution of the Mathieu equation is dependent on parameters, and the approximate solution can determine the dynamic resonant output of the resonant gyroscope. Hence, it is of interest to characterize the dynamic characteristic of the resonant gyroscope by the approximate solution of the Mathieu equation.

3. Approximate solution of the Mathieu equation

Since the input into the resonant gyroscope is modulated by a periodic function, its output must be demodulated into a stable state, and the solution of the parametric excitement equation (11) must be in its stable regions.

For the resonant gyroscope, with limitations of parameters δ and ε, an approximate solution can be derived in its stable regions and obtained by the small parameter perturbation method.

Let

$$q = {\rm e}^{\sqrt{\delta}\int w(z)\,{\rm d}z}, \tag{12}$$

where $w(z)$ is a differentiable function of z, then

$$\frac{{\rm d}q}{{\rm d}z} = \sqrt{\delta}w(z)\,{\rm e}^{\sqrt{\delta}\int w(z)\,{\rm d}z}, \tag{13}$$

$$\frac{{\rm d}^2q}{{\rm d}z^2} = \left(\sqrt{\delta}w'(z) + \delta w^2(z)\right){\rm e}^{\sqrt{\delta}\int w(z)\,{\rm d}z}. \tag{14}$$

Substituting the above equations into Eq. (11) yields

$$\left(\sqrt{\delta}w'(z) + \delta w^2(z)\right){\rm e}^{\sqrt{\delta}\int w(z)\,{\rm d}z} + (\delta + \varepsilon\cos 2z)\,{\rm e}^{\sqrt{\delta}\int w(z)\,{\rm d}z} = 0, \tag{15}$$

$$\frac{w'(z)}{\sqrt{\delta}} + w^2(z) + 1 + \beta\cos 2z = 0. \tag{16}$$

In Eq. (16), $\beta = \varepsilon/\delta = 2\varepsilon'/\delta' \leq 1$, and β can be naturally assumed to be small. If parameter β is defined as the small parameter, function $w(z)$ can be expanded in series of powers of β as follows:

$$w(z) = w_0 + \beta w_1 + \beta^2 w_2 + \cdots, \tag{17}$$

$$w'(z) = w_0' + \beta w_1' + \beta^2 w_2' + \cdots, \tag{18}$$

$$w^2(z) = \left(w_0 + \beta w_1 + \beta^2 w_2 + \cdots\right)^2 = w_0^2 + \beta(2w_0w_1)$$

$$+\beta^2\left(2w_0w_1+w_1^2\right)+\cdots. \tag{19}$$

Substituting Eqs. (17), (18), and (19) into Eq. (16) and gathering terms of the same order with respect to β, we obtain the following differential equations:

$$\begin{aligned}&\left(\frac{1}{\sqrt{\delta}}w_0'+w_0^2+1\right)\\&+\beta\left(\frac{1}{\sqrt{\delta}}w_1'+2w_0w_1+\cos 2z\right)\\&+\beta^2\left(\frac{1}{\sqrt{\delta}}w_2'+2w_0w_2+w_1^2\right)=0,\end{aligned} \tag{20}$$

$$\begin{cases}\dfrac{1}{\sqrt{\delta}}w_0'+w_0^2+1=0,\\ \dfrac{1}{\sqrt{\delta}}w_1'+2w_0w_1+\cos 2z=0,\\ \dfrac{1}{\sqrt{\delta}}w_2'+2w_0w_2+w_1^2=0.\end{cases} \tag{21}$$

Form Eq. (21), we have

$$\begin{cases}w_0=\tan\left(-\sqrt{\delta}z+C_1\right),\\ w_1=C_2\cos^2\left(-\sqrt{\delta}z+C_1\right)\\ \quad+\cos^2\left(-\sqrt{\delta}z+C_1\right)\\ \quad\times\int\sqrt{\delta}\cos 2z\cos^2\left(-\sqrt{\delta}z+C_1\right)\mathrm{d}z,\\ \quad\vdots\end{cases} \tag{22}$$

Substituting Eq. (22) into Eq. (17) yields a complicated approximate solution of the Mathieu equation, and it is not useful for analyzing the dynamic characteristics of the resonant gyroscope. Therefore, it is very important to choose a small parameter to obtain the approximate solution of the Mathieu equation.

Let $\sigma=\dfrac{1}{\sqrt{\delta}}$, if δ is very large, σ will be very small and σ may be defined as the small parameter. Therefore function $w(z)$ can be expanded in series of powers of σ as follows:

$$w(z)=w_0+\sigma w_1+\sigma^2w_2+\cdots, \tag{23}$$

$$w'(z)=w_0'+\sigma w_1'+\sigma^2w_2'+\cdots, \tag{24}$$

$$\begin{aligned}w^2(z)&=\left(w_0+\sigma w_1+\sigma^2w_2+\cdots\cdots\right)^2\\&=w_0^2+\sigma\left(2w_0w_1\right)+\sigma^2\left(2w_0w_1+w_1^2\right)\\&\quad+\cdots.\end{aligned} \tag{25}$$

Substituting Eqs. (23), (24), and (25) into Eq. (16) and gathering terms of the same order with respect to σ, we obtain the following differential equations:

$$\begin{aligned}&\sigma w'(z)+w^2(z)+1+\beta\cos 2z\\&=\sigma w_0'+\sigma^2w_1'+\sigma^3w_2'+w^2(z)+w_0^2+\sigma\left(2w_0w_1\right)\\&\quad+\sigma^2\left(2w_0w_2+w_1^2\right)+1+\beta\cos 2z\\&=w_0^2+1+\beta\cos 2z+\sigma\left(w_0'+2w_0w_1\right)\\&\quad+\sigma^2\left(w_1'+2w_0w_2+w_1^2\right)+\cdots\\&=0,\end{aligned} \tag{26}$$

$$\begin{cases}w_0^2+1+\beta\cos 2z=0,\\ w_0'+2w_0w_1=0,\\ w_1'+2w_0w_2+w_1^2=0,\\ \quad\vdots\end{cases} \tag{27}$$

From Eq. (27) it follows that

$$\begin{cases}w_0=\pm\mathrm{i}\mu,\\ w_1=-\dfrac{1}{2}\dfrac{\mu'}{\mu},\\ w_2=\pm\dfrac{\mathrm{i}}{8\mu^2}\left(3\mu'^2-2\mu\mu''\right),\\ \quad\vdots,\end{cases} \tag{28}$$

where $\mu^2=1+\beta\cos 2z$. Substituting Eq. (28) into Eq. (17), we obtain function $w(z)$ and the approximate solution of the Mathieu equation $q(z)$ as

$$\begin{aligned}w(z)&=\pm\mathrm{i}\mu-\frac{\sigma}{2}\frac{\mu'}{\mu}\pm\mathrm{i}\frac{\sigma^2}{8\mu^2}\left(3\mu'^2-2\mu\mu''\right)\\&=\pm\mathrm{i}\mu-\frac{1}{2\sqrt{\delta}}\frac{\mu'}{\mu}\pm\mathrm{i}\frac{1}{\delta}\frac{3\mu'^2-2\mu\mu''}{8\mu^2},\end{aligned} \tag{29}$$

$$\begin{aligned}&\int w(z)\,\mathrm{d}z\\&=\int\left(\pm\mathrm{i}\mu-\frac{1}{2\sqrt{\delta}}\frac{\mu'}{\mu}\pm\mathrm{i}\frac{1}{\delta}\frac{3\mu'^2-2\mu\mu''}{8\mu^2}\right)\mathrm{d}z+C\\&=\frac{1}{\sqrt{\delta}}In\mu^{-\frac{1}{2}}\pm\mathrm{i}\int\left(\mu+\frac{3\mu'^2-2\mu\mu''}{8\delta\mu^2}\right)\mathrm{d}z+C,\end{aligned} \tag{30}$$

$$\begin{aligned}q(z)&=\mathrm{e}^{\sqrt{\delta}\int w(z)\,\mathrm{d}z}=\exp\left(In\mu^{-1/2}\pm\mathrm{i}\int\sqrt{\delta}\mu\mathrm{d}z\right)\\&=A\mu^{-1/2}\exp\left(\pm\mathrm{i}\sqrt{\delta}\int\mu\,\mathrm{d}z\right)\\&=\frac{B}{\left(\delta+\varepsilon\cos 2z\right)^{1/4}}\\&\quad\times\cos\left(\int\left(\delta+\varepsilon\cos 2z\right)^{1/2}\mathrm{d}z+\theta\right),\end{aligned} \tag{31}$$

where A, B, and θ are arbitrary constants and are determined by the primal conditions. From Eq. (31), it is easy to see that there is an amplitude modulation at the same time as when the frequency modulation in the output of the resonant gyroscope takes place. In the resonant gyroscope under investigation, the resonant frequency shift in the sensing device is used to

sense the angular velocity, so the frequency of output signal of the resonant gyroscope is

$$\begin{aligned}\omega(z) &= \frac{\mathrm{d}\left(\int(\delta+\varepsilon\cos 2z)^{1/2}\,\mathrm{d}z+\theta\right)}{\mathrm{d}z}\\ &= (\delta+\varepsilon\cos 2z)^{1/2}, \qquad (32)\\ \omega(t) &= \frac{\omega_\mathrm{d}}{2}\sqrt{\delta+\varepsilon\cos\omega_\mathrm{d}t}\\ &= \sqrt{\delta'+2\varepsilon'\cos\omega_\mathrm{d}t}\\ &= \sqrt{\delta'}\sqrt{1+\beta\cos\omega_\mathrm{d}t}\\ &= \omega_0\sqrt{1+\beta\cos\omega_\mathrm{d}t}, \qquad (33)\\ \omega(t) &= \omega_0\sqrt{1+\beta\cos\omega_\mathrm{d}t}\\ &\approx \omega_0\left(1+\frac{\beta\cos\omega_\mathrm{d}t}{2}\right)\\ &= \omega_0+\frac{\varepsilon'}{\omega_0}\cos\omega_\mathrm{d}t, \qquad (34)\end{aligned}$$

where $z=\frac{\omega_\mathrm{d}t}{2}$ and $\omega_0=\sqrt{\delta'}$, with ω_0 being the no-load resonant angular frequency of DETF. From Eq. (33), it is easy to see that the change in tension along the DETF results in changes of the stiffness, shifting the resonant frequency. At the same time, the modulated power of the output resonant frequency is determined not only by modulated stiffness ε', but also by static modulated stiffness δ'.

The relation between the modulated frequency output and the input angular velocity is given by

$$\begin{aligned}\hat{\omega}(t) &= \frac{\varepsilon'}{\omega_0}\cos\omega_\mathrm{d}t=\omega_0 SF(t)\\ &= \omega_0 S\frac{m}{4}Q\omega_\mathrm{d}\Omega y_\mathrm{m}(t), \qquad (35)\end{aligned}$$

where y_m is the vibration amplitude of the proof mass. In order to obtain a linear output of the modulated frequency, some transformations in one period are applied to change Eq. (35) into

$$\begin{aligned}y_\mathrm{output} &= \int_T \hat{\omega}(t)\cdot y_\mathrm{m}(t)\,\mathrm{d}t\int_T y_\mathrm{m}^2(t)\,\mathrm{d}t\\ &= \int_T \frac{SmQ}{4}\omega_0\omega_\mathrm{d}\Omega y_\mathrm{m}(t)\cdot y_\mathrm{m}(t)\,\mathrm{d}t\Big/\int_T y_\mathrm{m}^2(t)\,\mathrm{d}t\\ &= \frac{SmQ}{4}\omega_0\omega_\mathrm{d}\Omega. \qquad (36)\end{aligned}$$

The dynamic frequency output characteristics of the resonant gyroscope based on the approximate solution of the Mathieu equation are obtained theoretically, which will be evaluated by the experimental date in the next section.

4. Simulation and experiment

4.1. Simulation

The numerical solution of Eq. (11) obtained by using the Runge–Kutta method can be used to validate the accuracy of the approximate solution (Eq. (31)) in the resonant gyroscope parameter range. Figure 3 shows that the amplitude is modulated by the change of the frequency in the parametric excitement system. When the DETF beam stiffness (the central line) reaches its maximal value, the frequency of the response signal also rises to its maximal value, while the amplitude decreases to its minimal value. The trends are reversed when the stiffness reaches its minimum, which proves that the amplitude modulation presents at the same time when the frequency modulation in the output of the resonant gyroscope takes place, and it also shows that the approximate solution Eq. (31) for the Mathieu equation is reasonable and presents the dynamic characteristic of the resonant gyroscope.

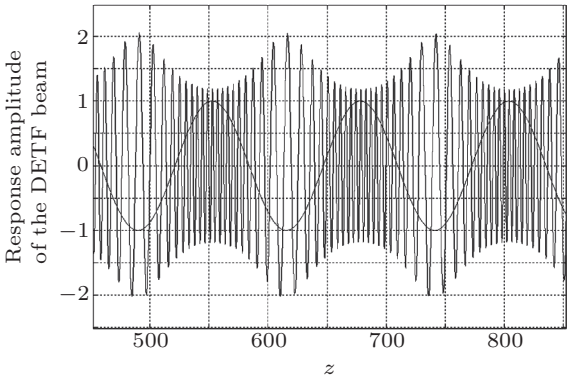


Fig. 3. Numerical solution of the Mathieu equation.

4.2. Experiment

The numerical simulation has shown that the numerical simulation result and the theoretical solution have the same dynamic output characteristic. In order to evaluate the approximate solution for the Mathieu equation experimentally, some relevant experiments are carried out.

The resonant gyroscope shown in Fig. 4 is made by Taiyuan Aeroinstuments CO. Ltd. and will be used as the sensor to be calibrated. The resonant frequency of the proof mass is around 30 Hz, and the resonant frequency of the DETF is around 1 kHz. The resonant gyroscope parameters are listed in Table 1.

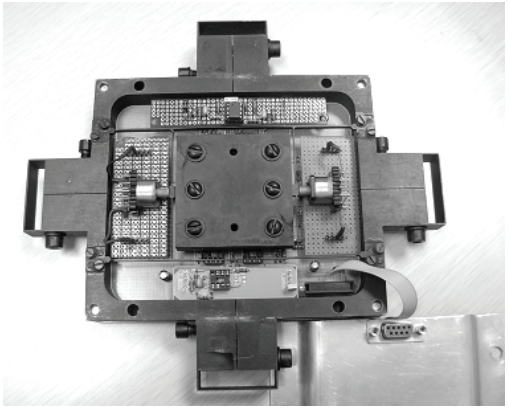


Fig. 4. The resonant gyroscope made by Taiyuan Aeroinstuments CO. Ltd.

Table 1. Parameters of the resonant gyroscope for experiment.

Symbol	Description	Values
ρ	density	7.8×10^3 kg/m^3
E	Young's modulus	2×10^{11} P
m	proof mass	0.261495 kg
L	DETF beam length	0.062 m
I	area moment of inertia of the DETF beam	4.159375×10^{-2} mm^4
Q	quality factor	100

The resonant gyroscope shown in Fig. 5 has a standard angular velocity in the range from -200 °/s to 200 °/s. The calibration system is composed of three parts, i.e., a resonant gyroscope, a rate table (CIMM00003719), and a signal sampling device. The resonant gyroscope can be used to detect the rotations produced by the rate table. The rate table can rotate at a series of angular velocities, and the angular velocities are applied to the resonant gyroscope. The direct output signal of the resonant gyroscope is sampled every 20 s by the signal sampling device. The sampled crude signal at a fixed angular velocity (100 °/s) is shown in Fig. 6. The proof mass vibrating signal is shown in Fig. 6(a), and the beam original output signal is shown in Fig. 6(b). As shown in Fig. 6, the output of the resonant gyroscope beam is not a linear frequency output. Under the condition of transformed output in Eq. (36), the ratio between the alternating part of the frequency output and the changing angular velocity is plotted in Fig. 7. As shown in Fig. 7, the resonant gyroscope beam output frequency is a linear output, which is very close to the theoretical result, i.e., the transformed result in the foregoing section. The theoretical curve and the experimental data coincide perfectly, which means that the approximate solution of the Mathieu equation can present the dynamic output characteristic of the resonant gyroscope.

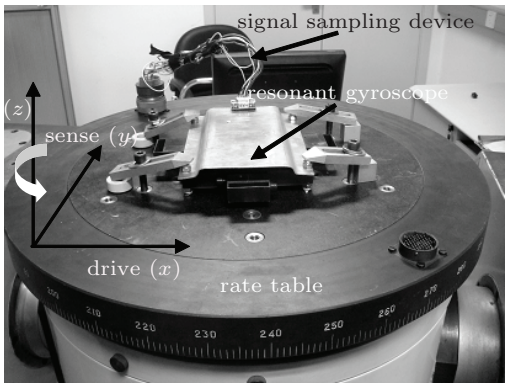


Fig. 5. Calibration assembly of the resonant gyroscope.

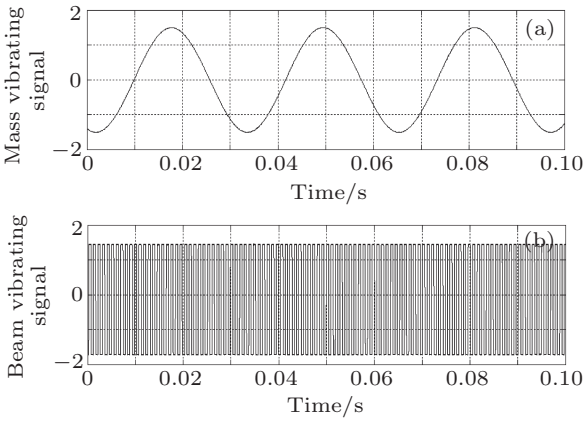


Fig. 6. (a) Mass vibrating and (b) beam original output signals from the resonant gyroscope.

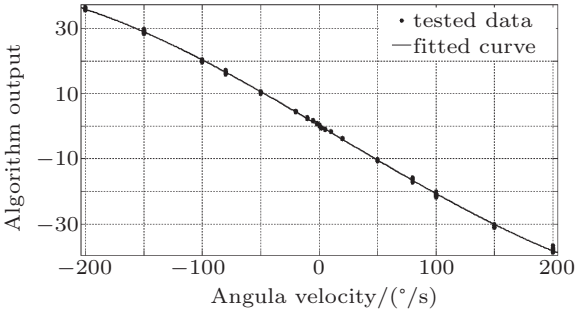


Fig. 7. Fitting result of the output frequency response date for changing angular velocity.

5. Conclusions

In this paper, the dynamic characteristic of the resonant gyroscope with alternating acceleration has been studied, which shows that the resonant gyroscope is equivalent to a parametric resonant system and can be described by the Mathieu equation. The approximate relationship between the resonant gyroscope parameters and the Mathieu equation is studied.

An approximate analytical method based on the small parameter perturbation is employed to investigate the approximate solution of the Mathieu equation. The benefits of using the Mathieu equation to describe the parametric resonance dynamic characteristic of the resonant gyroscope are analyzed theoretically and studied experimentally. Numerical simulations are carried out for investigating the dynamic output performance. A very good agreement between the simulation results obtained by the numerical integration and the analytical solution is observed. Experiments are also carried out for investigating the dynamic output performance. A very good agreement is obtained between the results obtained experimentally and analytically. Therefore, it is found that it is very useful to analyze the dynamic characteristic of the resonant gyroscope by using the Mathieu equation approximate solution.

References

[1] Seshia A A 2002 *Integrated Micromechanical Resonant Sensors for Inertial Measurement Systems* (Ph. D. dissertation) (Berkeley: University of California at Berkeley)

[2] Acar C and Shkel A M 2004 *Journal of Micromechanics and Microengineering* **14** 15

[3] Yang J B, Jiang L J and Chen D C 2004 *Journal of Sound and Vibration* **274** 863

[4] Mohite S, Patil N and Pratap R 2006 *Journal of Physics* **34** 757

[5] Mahmoodi S N, Jalili N and Khadem S E 2008 *Journal of Sound Vibration* **311** 1409

[6] Seshia A A, Howe R T and Montague S 2002 *Proceeding of the 15th IEEE Int. Conf. MEMS*, January 20–24, 2002 Las Vegas, USA, p. 722

[7] Moussa H and Bourquin R 2006 *IEEE Sensors Journal* **6** 310

[8] Jeong C, Seok S, Lee B, Kim H and Chun K 2004 *J. Micromech. Microeng.* **14** 1530

[9] Gallacher B J, Burdess J S and Harish K M 2006 *J. Micromech. Microeng.* **16** 320

[10] Park S, Tan C W, Kim H and Hong S K 2009 *Sensors* **9** 5952

[11] Sammarco P, Tran H H, Gottlieb O and Mei C C 1997 *J. Fluid Mech.* **15** 327

[12] Vittori G 1998 *J. Hydraul. Eng.* **4** 124

[13] Poulin F J, Flierl G R and Pedlosky J 2003 *J. Fluid Mech.* **481** 329

[14] Pedlosky J and Thomson J 2003 *J. Fluid Mech.* **490** 189

[15] McLachlan N W 1964 *Theory and Application of Mathieu Function* (New York: Dover Publicatons Inc) pp. 90–95

[16] Liu S S and Liu S D 2002 *Special Function* (Weather Publicatons Inc) pp. 737–739 (in Chinese)

[17] Harris C and Crede C 1976 *Shock and Vibration Handbook* (2nd Edn.) (New York: Mc-Graw Hill) pp. 1–13

[18] Wang Y Z and Zhou Y Z 2011 *Chin. Phys.* B **20** 040501

[19] Francis J P and Glenn R F 2008 *Proc. R. Soc.* A **464** 1885

[20] Coisson R, Vernizzi G and Xiao K Y 2009 *Proceeding of the International Workshop on Open-source Software for Scientific Computation* (OSSC), September 18–20, 2009 Guiyang, China, p. 3

[21] Rand R H, Sah S M and Suchorsky M K 2010 *Commun. Nonlinear Sci. Numer. Simulat.* **15** 3254

[22] http://www.taihangybc.com